LMFBR-FUEL CLADDING THERMAL CREEP STRAIN UNDER LINEARY INCREASING INTERNAL PRESSURE

M. NAKATSUKA

Nuclear and Electrical Laboratory, Toshiba Research and Development Center, Tokyo Shibaura Electric Company, Ltd.; 1, Komukai Toshiba-cho, Saiwai-ku, Kawasaki City, Kanagawa, 210, Japan

SUMMARY

In the LMFBR fuel design, it is important to evaluate the accumulated thermal creep strain and time to rupture, reasonably. In the past, most of the creep data available for the estimation of the thermal creep and time to rupture of fuel cladding originate from conventional tensile constant load tests. However, in service, fuel claddings are subjected to almost linearly increasing internal pressure, due to the accumulation of fission product gas. It is often the case that uniaxial data are not correctly applied to a biaxial situation.

This paper describes an apparatus designed to simulate the continuously increasing internal pressure due to the accumulation of fission product gas. There is also an examination of the effects of increasing pressure on the thermal creep rate of cladding. Test specimens are 20% C.W. type 316 stainless steel tubes with 6.5 mm OD, 5.6 mm ID and 200 mm length. Increasing pressure creep tests were performed at 700°C, the hoop stress was increased in steps with 3 incremental rates of 0.15, 0.075 and 0.0375 kg/mm²h. Constant pressure creep tests were also performed at the same temperature for comparison.

As mentioned above, calculations of creep behavior under increasing stress are normally made using the stationary creep rate obtained from constant pressure tests. Thus, it is important to know these creep rates agree with creep rates directly measured from strain-time plot under increasing pressure. The results show that the creep rates obtained from creep curves under increasing pressure are several times as high as the stationary creep rates measured under the same constant pressure. Creep strain rate under increasing pressure, due to the accumulation of gaseous fission products in the actual fuel cladding, is approximately 2 to 5 times that of the constant pressure creep rates, although the creep rate magnification depends on the stress and the stress-increase rate.

Based on so-called time hardening theory and strain hardening theory, creep strain rate under increasing pressure is calculated using the strain-time plot under constant pressure. The calculated creep strain rate agrees very well with that obtained under increasing pressure. Based on the results mentioned above, it is concluded that, in the fuel design, evaluation of the actual fuel cladding thermal creep strain, based on the stationary creep rate obtained from constant pressure tests, will give a lower estimate. Therefore, a creep constitutive equation, obtained from constant pressure tests, should include primary creep as well as stationary creep.

1. Introduction

The life time of Liquid Metal Fast Breeder Reactor (LMFBR) fuel pin is strongly affected by the fuel cladding high temperature properties. Especially, fuel cladding creep properties plays an important role in determining the burn up of fuel subassembly. There are a number of reports [1] dealing with the fuel pin, but most of the creep data determination experiments were carried out under constant pressure. These data are usually analyzed in terms of steady state creep [2]. In design method currently in use [3], fuel cladding thermal creep estimation has been made with data obtained from these tests. However, in service, fuel claddings are subjected to almost linearly increasing internal pressure, due to the accumulation of fission product gas.

Therefore, it is necessary to investigate the effect of the increasing pressure on the thermal creep strain rate. B. Blanc [4] and H. Böhm [5] investigated their effect under uniaxial loading conditions. However, as is often the case in creep strain prediction, uniaxial data are not correctly applied to the biaxial situation. The authors are not aware of any investigation, where such experiments have been carried out under internal gas pressure loading.

This paper describes an apparatus designed to simulate the increasing pressure due to the accumulation of fission product gas. The specific purpose of the apparatus was the measurement of creep strain under increasing pressure. These creep data, obtained on LMFBR fuel claddings, are compared with steady state creep under constant pressure tests. There is also application of these test results to typical LMFBR fuel design.

2. Equipment Description

The apparatus consists of an electric furnace, a high-pressure gas system, associated pressure increasing equipment, and electronic devices for pressure and furnace temperature control. Specimen pressure and temperature and test duration are continuously monitored while being recorded. Tests can be conducted in either air or inert-gas environment.

The high-pressure piping arrangement is shown in Fig. 1. Argon gas is used as the pressurizing media, because it prevents the specimen corrosion. Argon gas is compressed by the diaphragm compressor and is accumulated in a high-pressure gas storage vessel. Constant volume gas, which flows through the pressure regulator, is charged by a compressor intermittently,to increase the specimen pressure. Any pressure increasing rates can be obtained by adjusting the volume of variable volume gas storage vessel and electric timer. Specimen pressures are monitored or recorded by a 6-inch diameter precision pressure gage and pressure temperature. The furnace chamber is 50 mm ID Type 304 stainless steel tube. It is heated by a three zone, electric tube furnace. Each zone is powered by a silicon-controlled rectifier.

3. Specimen Preparation

Standard specimen design is shown in Fig. 2, which is 20% C.W. Type 316 stainless steel tube with 6.5mm OD, 5.6mm ID and 200mm length. Most of the specimen volume is displaced with a solid rod. The top end and high pressure gas inlet are TIG welded. The test specimen is given a thorough nondestructive inspection by ultrasonic techniques. The initial inside and outside diametral inspection of the 200mm specimen length is made with air gages. Standard deviation in outer diameter and wall-thickness are less than 0.1% and 1%, respectiveiy. The chemical composition and room-temperature mechanical properties of the steel used in this investigation is given in Table I.

4. Increasing Pressure Creep Tests

Up to four specimens in a furnace chamber can be connected to a high-pressure gas source. The 700°C test temperature was chosen because earlier results showed and many creep data were more pronounced at 700°C. Three temperature measurements were made for each specimen along the specimen length. Temperature control was held within ±2°C, with a uniform temperature zone more than 90mm in length.

Two specimens are connected to the same pressure source. They are brought to test temperature in about 4 hours. The creep test is initiated by starting the mechanical pump provided for pressure increasing. Argon gas is chosen as pressurizing media. The increasing pressure creep tests were interrupted for diametral measurements. Diametral measurements are made to the nearest ±2 μm with a digital electric micrometer at room temperature after specimen depressurization.

Six measurements were made at each 20mm interval along the specimen length. Average values were used to determine the diametral strain. On resumption of the test, specimens were pressurized to about 50% of the accumulated pressure during heating. This procedure retains the microstructure corresponding to the accrued strain history before shutdown [6,7]. The amount of diametral strain that occurs at this pressure during the 4 hr heating period is small, compared with that during hundreds of full test periods.

Three pressure increasing rates, 0.15, 0.075 and 0.0375 kg/cm^2·hr, were used. Resulting rates give a circumferential stress increasing rate of 1.01×10^{-2}, 5.04×10^{-3} and 2.52×10^{-3} kg/mm^2·hr, using the average radius equation. Constant pressure creep tests were also performed at the same temperature for comparison.

5. Test Results and Discussion

Creep strain under constant loading can be written as

$$\epsilon_c = A\sigma^n t^m \qquad (1)$$

$$n = \alpha\sigma^2 + \beta\sigma + \gamma \qquad (2)$$

where, ϵ_c is circumferential strain and A, n and m are material constants. Preliminary constant pressure creep tests were conducted at 700°C to determine the following creep constants in eq. (1) and eq. (2).

$$A = 2.76 \times 10^{-5}$$

$$n = 8.579 \times 10^{-2}\sigma^2 - 6.894 \times 10^{-1}\sigma + 3.4723$$

$$m = 1.1745$$

Stress-steady state creep strain rate curve is shown in Fig. 3. Circumferential creep strain curve with three pressure increasing rates of 0.15, 0.075, 0.0375 kg/cm^2·Hr (1.01×10^{-2}, 5.04×10^{-3}, 2.52×10^{-3} kg/mm^2·Hr) is shown in Fig. 4. Two or three test specimens are creep tested at the same time for each pressure increasing rate. Creep strains under the increasing pressure are best fitted with higher order polynomial, to lead the creep strain rate by the differentiation. These creep strain rates are shown in Fig. 5. The figures also contain, for comparison, the steady state creep rate already shown in Fig. 3. As can be seen from Fig. 5, creep rates under increasing pressure are greater than the steady state creep rates at the same stress levels.

Based on eq. (1), a creep rate under increasing pressure is described by

$$\dot{\epsilon}_c = m A \sigma^n t^{m-1} \tag{3}$$

$$\dot{\epsilon}_c = m A^{\frac{1}{m}} \sigma^{\frac{n}{m}} \epsilon_c^{\frac{m-1}{m}} \tag{4}$$

by means of time hardening and strain hardening theories, respectively. Maximum creep strain rate under increasing stress with a constant stress rate $\dot{\sigma}$ will be given by the following equation, which corresponds to total strain assumption.

$$\dot{\epsilon}_c = m A \sigma^n t^{m-1} + A\sigma^n\{(2\alpha\sigma + \beta)\ln\sigma + \frac{n}{\sigma}\}\dot{\sigma} t^m \tag{5}$$

Creep strain at each time and stress level can be calculated by substituting eq. (3), (4) or (5) into the following equation.

$$\epsilon_c = \int_0^t \dot{\epsilon}_c \, dt \tag{6}$$

A number of papers have explained the creep behaviour under variable loading with strain hardening assumption [8]. It may be seen that total-strain theory is not a reasonable hypothesis. Nevertheless it is included here, for two reasons. Firstly, when used in component analysis, it gives a good approximation to a more realistic behaviour [9]. Secondly, for smoothly varying stress histories, total-strain theory forms a good approximation to complex theories of the hereditary type [10, 11, 12]. These two theories are applied to the analysis.

Figure 6 compares the creep data obtained under the increasing pressure with the calculated strain, based on strain hardening and total strain assumptions. The results

indicate that the strain hardening theory is close to the experimental data in the region up to 0.2 % creep strain. In the smaller increasing rate and longer time, test results show greater strain, however. On the other hand, total strain theory gives a good approximation in the longer time region. It seems that these changes in creep properties is caused mainly by the microstructure change, such as thermal recoverly, of the material.

Calculated creep strain rate, based on total strain theory and experimental results, are normalized with steady state creep strain rate already shown in Fig. 4. They are plotted in Fig. 7 as normalized creep rate versus stress increasing rate. It can be seen that experiment and theory give a relatively good agreement, taking into consideration large scatter commonly found in creep measurement. Figure 7 shows that creep rate for typical LMFBR fuel cladding will be about 2 to 5 times the steady state creep rate.

6. Application to LMFBR Fuel Design

Robinson's life fraction rule [13] is applicable for predicting rupture life under variable loading. Results are used in the design code at elevated temperature [14]. On the other hand, the accumulated strain has to be restricted within ductility, also.

As mentioned above, it was found that the strain hardening theory can be fitted to the experimental data in the range up to 0.2 % strain. Therefore, the creep constitutive equation, used in fuel pin analysis, has to include a transient creep as well as steady state creep.

However, for the fuel design, only steady state creep data are available, so far. It is important to develop a simplified method, using this available data, for fuel cladding strain assessment. It can be seen from Fig. 7 that creep rate under the increasing stress is obtained by multiplying steady state creep rate by a proper constant.

As an example, hoop stress is about 3.5 kg/mm^2 when about 1 % strain is reached at a stress increasing rate of 2.52×10^{-3} $kg/mm^2 \cdot Hour$. As can be seen from Fig. 7, creep rate under the increasing stress is nearly 2 times the steady state creep rate. Steady state creep rate is multiplied by 2 to consider the effect of increasing stress. These results are shown in Fig. 8. According to these figures, it is found that the conventional design method, based on steady state creep rate underestimates the creep strain, on the other hand multiplying proper constant based on total strain theory gives rather reasonable strain. The latter calculation method will be an acceptable design method for use in LMFBR fuel design, because it needs only conventional steady state creep rate.

7. Summary and Conclusions

Most of the creep data applicable to estimation of thermal creep strain in LMFBR fuel cladding originates from conventional tensile constant load tests. However, in service, fuel claddings are subjected to almost linearly increasing internal pressure, due to the accumulation of gaseous fission products.

This paper describes an apparatus designed to simulate the continuously increasing

internal pressure due to the accumulation of fission products gas. There is also an examination of the effect of increasing pressure on the thermal creep rate of 20 % cw type 316 stainless steel cladding. Steady state creep rate under constant pressure was compared with creep rate directly measured from strain-time plot under increasing pressure.

The test results indicate that strain hardening theory agrees well with the experimental data in the region up to 0.2 % creep strain. On the other hand, total strain assumption gives a good approximation in the region of smaller stress increasing rate and longer time. The results also show that creep rates under increasing pressure are several times as high as the steady state creep rates measured under the same constant pressure.

From the discussion above, creep strain rate in the typical LMFBR fuel cladding is approximately 2 to 5 times that of the steady state creep rates, although creep rate magnification depends on stress and stress increasing rate.

It is concluded that the conventional design method based on steady state creep rate underestimates the creep strain. Therefore, a creep constitutive equation should include transient creep as well as steady state creep. Instead of using a rather complex creep constitutive equation, the modified design method for use in LMFBR fuel design is also shown.

Acknowledgments

The technical advice and support of T. Kawada, Y. Kumaoka and E. Fujii are gratefully acknowledged.

References

[1] D. F. ATKINS, "Stress-Rupture Behavior of Types 304 and 316 Stainless Steel Cladding in High-Temperature Static Sodium", AI-AEC-12976 (Sept. 1970).

[2] F. GAROFLO, "Fundamentals of Creep and Creep-Rupture in Metals", MacMillan Co., New York (1965).

[3] E. G. STEVENS, "FFTF Fuel Pin and Subassembly Conceptual Design Methods and Data", BNWL-1064 (June 1970).

[4] B. BLANC et al., "Etude des Deformations de Fluage sous Solliciations Complexes D'un Acier Inoxydable Austenitique-Fluage sous Charge Progressive a Haute Temperature-Fluage sous Contrainte Thermique", IAEA/SM-173/4, Bruxelles, 1973.

[5] H. BÖHM et al., "Creep Rupture Behavior of a Neutron Irradiated 15/15 CrNiMoTiB Steel under Constant and Increasing Load, IAEA/SM-173/23, Bruxelles, 1973.

[6] J. B. CONWAY and P. N. FLAGELLA, "Physical and Mechanical Properties of Reactor Materials", GEMP-727 (Dec. 1969).

[7] F. L. YAGGEE et al., "Semiautomatic Apparatus for Creep and Stress-Rupture Tests of Thin-Wall Fuel-Cladding Tubes under Internal Gas-Pressure Loading", ANL-7801 (Sep. 1971).

[8] A. P. BORESI and O. M. SIDEBOTTOM, "Creep of Metals under Multiaxial States of Stress", Nuclear Engineering and Design 18 (1972).

[9] MARRIOTT, D. L. "Approximate Analysis of Transient Creep Deformation", J. Strain Analysis (1968) 3.

[10] RABOTNOV, Y. N. "Some Problems of the Theory of Creep", Tech. Notes natn. advis. Comm. Aeronaut., Wash. 1353 1953.

[11] GRAHAM, A. et al., "Relations Between Long and Short Term Properties of a Commercial Alloy", J. Iron Steel Inst. 1955 179.

[12] D. L. MARRIOTT et al., "Strain Accumulation and Rupture during Creep under Variable Uniaxial Tensile Loading", J. Strain Analysis 8 No. 3 (1973).

[13] ROBINSON, E. L., Trans. ASME60 (1938) 253.

[14] ASME Boiler and Pressure Vessel Code, Case-1592 (1974).

TABLE I. Compositions and room-temperatures mechanical properties of specimen

Material											
Contents (%)	C	Si	Mn	P	S	Ni	Cr	Mo	Co	B	N
	0.061	0.68	1.69	0.011	0.006	13.83	17.48	2.24	0.03	0.0003	0.0006

Room - temperature properties				
	U.T.S. kg/mm²	Y.S. kg/mm²	Elong. %	Hardness (HV)
	83.4	74.5	21.9	~285

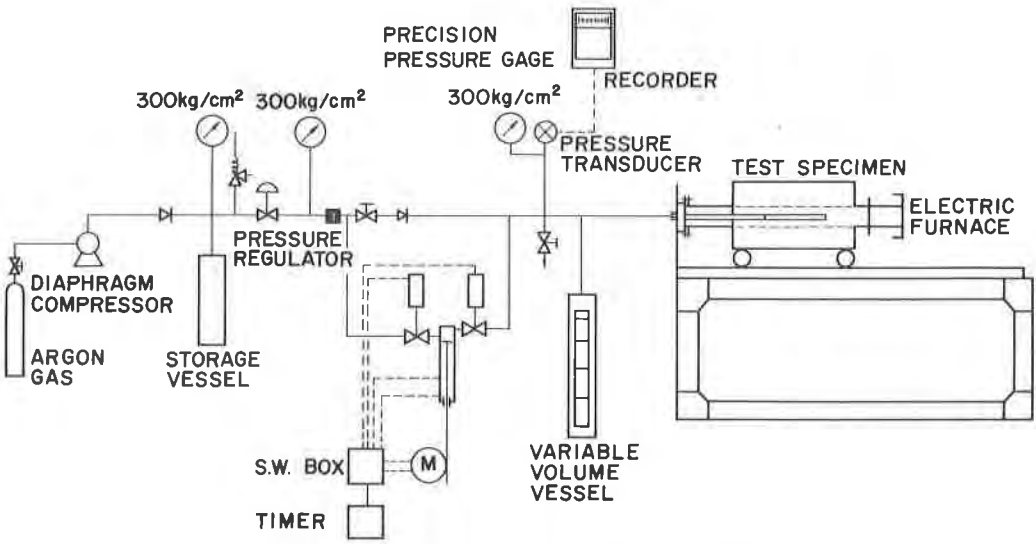

Fig. 1. Apparatus for increasing pressure creep tests.

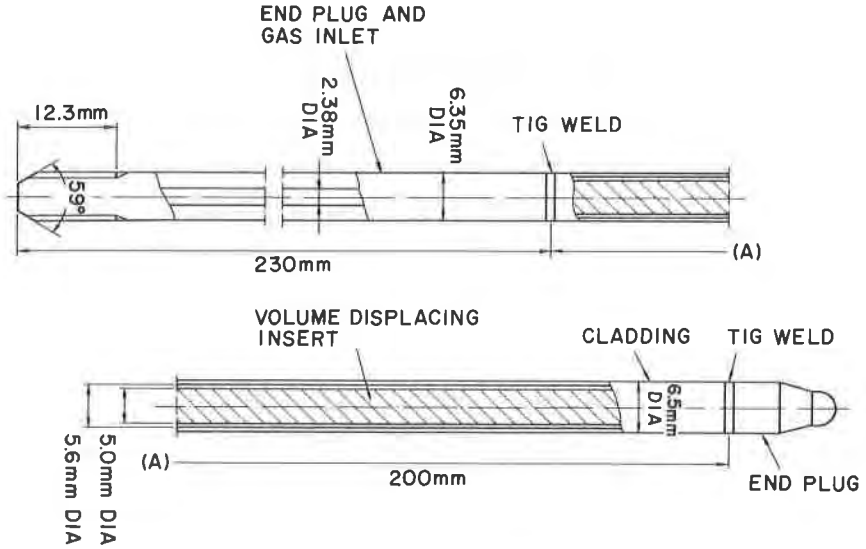

Fig. 2. Test specimen.

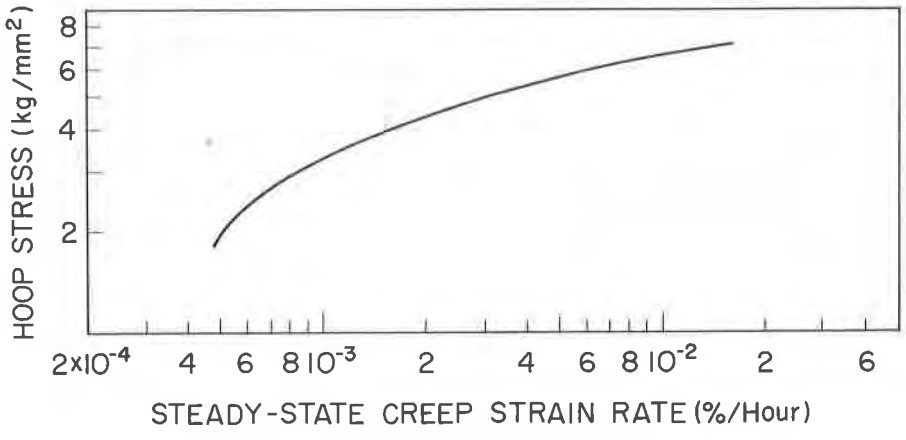

Fig. 3. Stress-steady state creep rate curve.

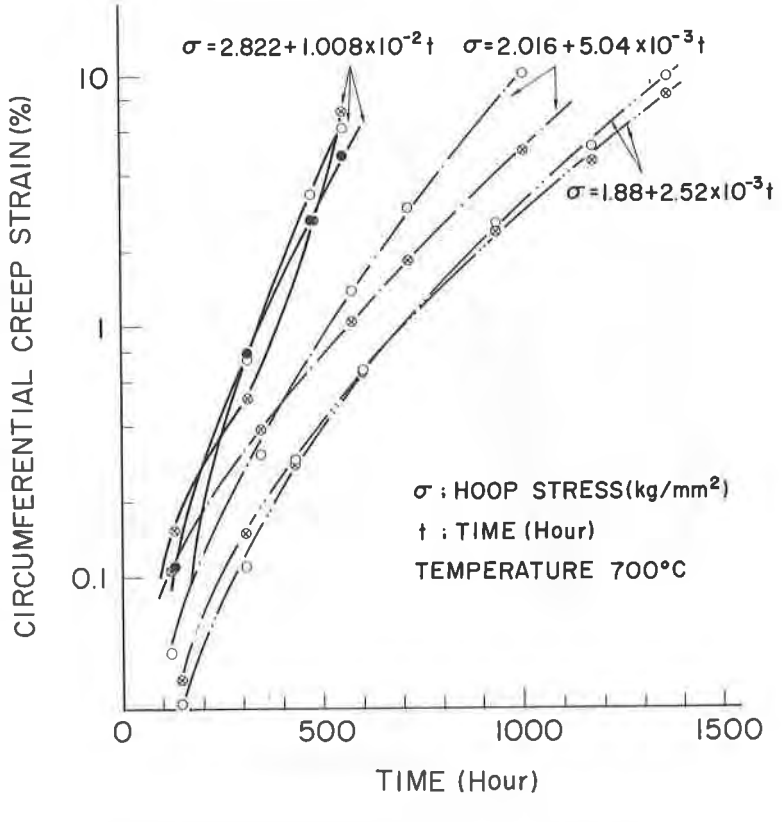

Fig. 4. Creep under increasing pressure at 700°C.

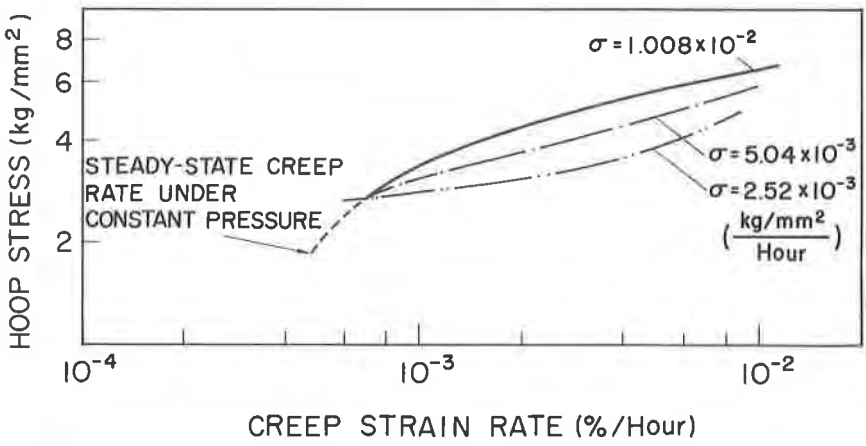

Fig. 5. Creep rate comparison under constant pressure and creep rates under increasing pressure tests at 700°C.

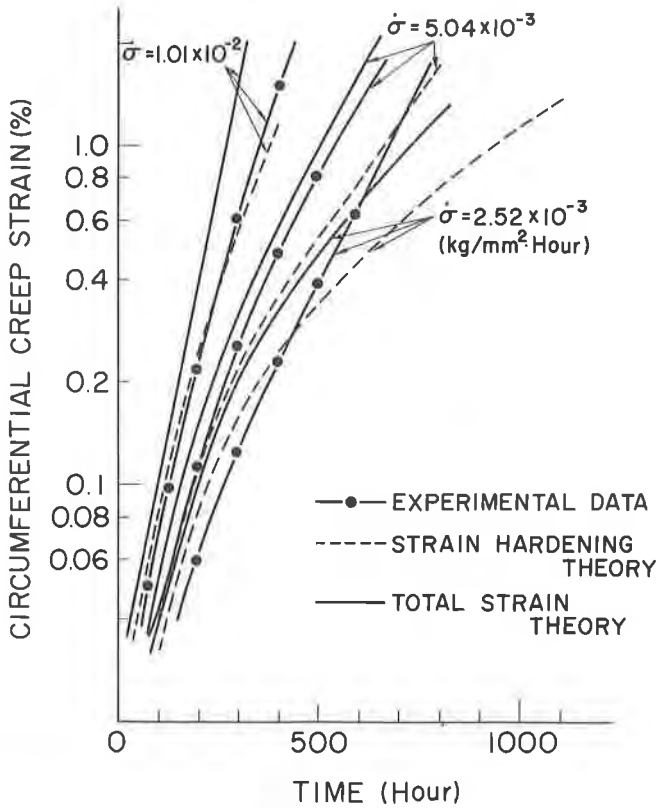

Fig. 6. Creep strain comparison under increasing pressure with creep strain calculated from constant pressure tests.

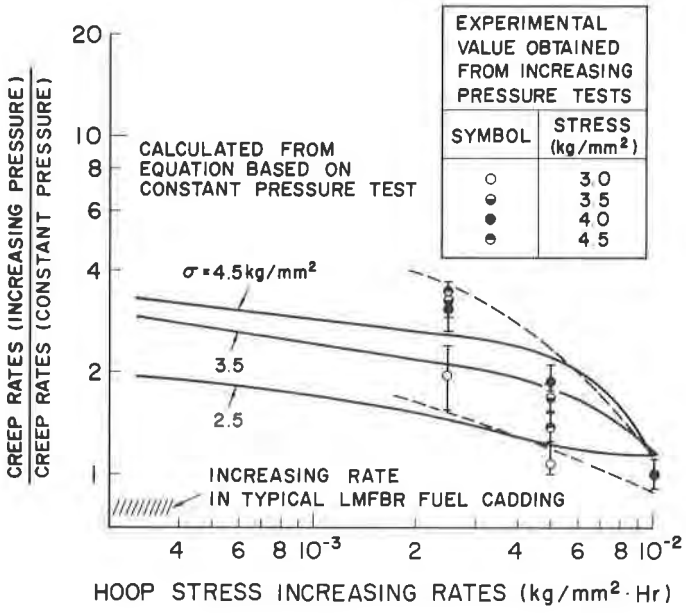

Fig. 7. Relations between creep rates under increasing pressure and hoop stress increasing rates.

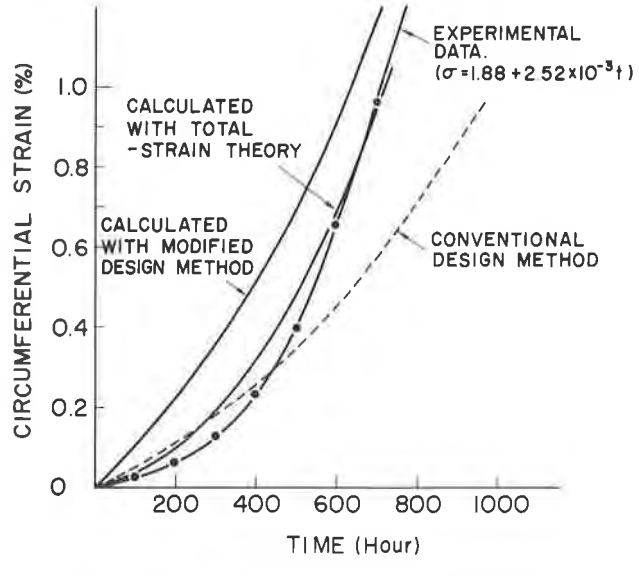

Fig. 8. Calculated strain with experiment comparison.